J|A|C|S COMMUNICATIONS

Published on Web 07/27/2010

Self-Confirming "AND" Logic Nanoparticles for Fault-Free MRI

Jin-sil Choi,[†] Jae-Hyun Lee,[†] Tae-Hyun Shin,[†] Ho-Taek Song,[‡] Eung Yeop Kim,[‡] and Jinwoo Cheon*,[†]

Department of Chemistry, Yonsei University, Seoul 120-749, Korea and Department of Radiology and Research Institute of Radiological Science, College of Medicine, Yonsei University, Seoul 120-752, Korea

Received May 24, 2010; E-mail: jcheon@yonsei.ac.kr

Abstract: Achieving high accuracy in the imaging of biological targets is a challenging issue. For MRI, to enhance imaging accuracy, two different imaging modes with specific contrast agents are used; one is a T1 type for a "positive" MRI signal and the other is a T2 type for a "negative" signal. Conventional contrast agents respond only in a single imaging mode and frequently encounter ambiguities in the MR images. Here, we propose a "magnetically decoupled" core−shell design concept to develop a dual mode nanoparticle contrast agent (DMCA). This DMCA not only possesses superior MR contrast effects but also has the unique capability of displaying "AND" logic signals in both the T1 and T2 modes. The latter enables self-confirmation of images and leads to greater diagnostic accuracy. A variety of novel DMCAs are possible, and the use of DMCAs can potentially bring the accuracy of MR imaging of diseases to a higher level.

By combining complementary information obtained from various imaging methods, including magnetic resonance imaging (MRI), positron emission tomography (PET), computed tomography (CT), and optical microscopy, multimodal imaging techniques have been devised to increase the accuracy of disease diagnosis.[1] However, even when multimodal techniques are employed, inherent problems still exist. For example, image matching difficulties caused by relocating biological samples and the discrepancies resulting from different depth penetrations and spatial/time resolutions of multiple imaging devices can lead to inaccuracies. Therefore, the development of dual imaging strategies that employ a single instrumental system can be an attractive solution.

MRI is a powerful technique for tomographic images of biological targets in a noninvasive manner with a high spatial resolution. In MRI, the relaxation time of protons of water in the sample is measured. Contrast agents are employed to greatly change proton relaxation rates and to enhance visualization of the differences between normal and disease tissues. T1 contrast agents, comprised typically of paramagnetic materials such as Gd complexes and Mn oxide nanoparticles, facilitate the spin−lattice relaxation of protons causing a positive (or bright) MR image.[2,3] On the other hand, T2 contrast agents that commonly consist of superparamagnetic nanoparticles (e.g., iron oxide) cause protons in their vicinity to undergo spin−spin relaxation which gives rise to negative (or dark) MR images.[3,4] Even so, such single mode contrast agents are not yet perfect and increasingly facing challenges especially when accurate imaging of small biological targets is needed.[5]

A dual mode strategy for MRI, where two different T1 and T2 imaging modes are utilized simultaneously, can potentially give highly accurate information. For such purposes, ultrasmall superparamagnetic iron oxide (USPIO), which displays enhanced T1 contrast effects, has been developed, but their T2 contrast effects are weak.[6] Although a system comprised of FeCo nanoparticles is the most representative one reported thus far that exhibits high T1 and T2 contrast effects,[7] an understanding of the mechanism by which this system operates is still unclear. The difficulty associated with the design of well-defined T1 and T2 dual mode contrast agents is related in part to the fact that, in the case of their direct contact, the magnetic field generated by a superparamagnetic T2 contrast material perturbs the relaxation process of the paramagnetic T1 contrast material (Figure 1a). This phenomenon induces the undesirable quenching of the T1 signal. Until now, a rational design concept of dual mode MRI contrast agents has not been proposed.

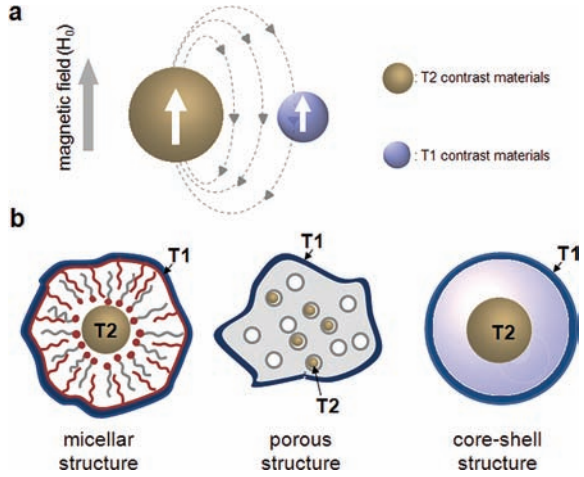

Figure 1. Magnetic coupling between T1 and T2 contrast materials and the structures for a dual mode nanoparticle contrast agent (DMCA). (a) Electronic spins of paramagnetic T1 contrast materials are affected by a magnetic field from superparamagnetic T2 contrast materials when they are in close proximity. (b) Three possible structures for a dual mode nanoparticle contrast agent with separating layers to prevent magnetic coupling between them.

In our studies described below, we have led to the development of a new T1−T2 dual mode nanoparticle contrast agent (DMCA). Organic block copolymers that form micellar structures, inorganic porous materials, such as MCM-48 that produces porous structures, and inorganic materials that generate core−shell structures are potential frameworks for construction of T1−T2 DMCAs (Figure 1b). Here, we selected T1−T2 DMCA that has inorganic core−shell structured particles, in which the T2 contrast material is located in the core and the T1 contrast material is positioned on the shell. By inserting a thickness-tunable separating layer, the magnetic coupling between the T1 and T2 materials can be modulated so that conditions for simultaneous generation of strong T1 and T2 contrast effects can be found. The T1 contrast material is positioned on the shell of the particles so that it is in direct contact with water.'[8] On the other hand, the superparamagnetic T2 contrast material is situated

[†] Department of Chemistry.
[‡] Department of Radiology.

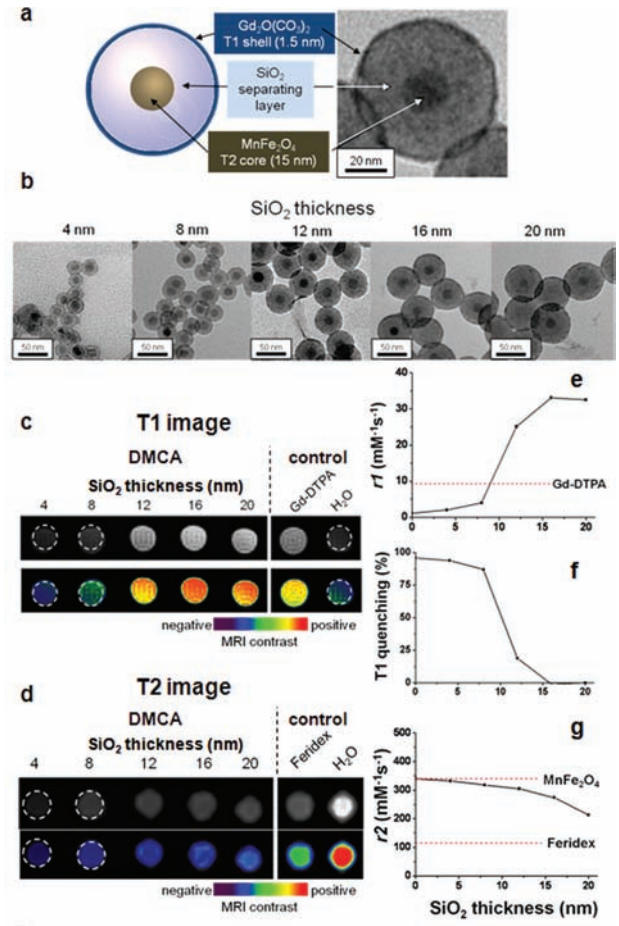

h

SiO_2 thickness (nm)	DMCA[1] 4	8	12	16	20	$MnFe_2O_4$[2]	T1 contrast agent Gd-DTPA[2]	T2 contrast agent Feridex[2]
r1 ($mM^{-1}s^{-1}$)	2.0	4.0	25.1	33.1	32.5	1.1	9.6	11.5
r2 ($mM^{-1}s^{-1}$)	332	318	305	274	213	340	8.5	108

1. *r1*: $mM^{-1}s^{-1}$ (Gd), *r2*: $mM^{-1}s^{-1}$ (Mn+Fe) 2. *r1* and *r2* are based on metal concentration.

Figure 2. T1 and T2 MR imaging of DMCA with a separating layer of SiO_2. (a) Schematic and transmission electron microscope (TEM) image of core−shell type DMCA [$MnFe_2O_4$@SiO_2@$Gd_2O(CO_3)_2$]. (b) TEM images of DMCA with variable separating layer thickness (4, 8, 12, 16, and 20 nm), having a fixed $MnFe_2O_4$ core (15 nm in diameter) and a $Gd_2O(CO_3)_2$ shell (1.5 nm). (c) T1- and (d) T2-weighted MR images and their color coded images of DMCA with varying SiO_2 thickness by using 4.7 T MRI. Contrast agents: 200 μM (Gd) for T1 image, 100 μM (Mn + Fe) for T2 images. The images of Gd-DTPA and Feridex were taken together for the purpose of comparison. In the color coded image, positive and negative contrasts were indicated by the red and blue color, respectively. (e) Graph of *r1* vs SiO_2 thickness. (f) Graph of T1 quenching vs SiO_2 thickness [T1 quenching (%) = $\{(r1_{SiO_2@GdO_2(CO_3)_2} - r1_{DMCA})/r1_{SiO_2@Gd_2O(CO_3)_2}\} \times 100$, $r1_{SiO_2@Gd_2O(CO_3)_2} = 31$ mM^{-1} s^{-1} (Table S1)]. (g) Graph of *r2* vs SiO_2 thickness. (h) *r1* and *r2* of DMCA, $MnFe_2O_4$, Gd-DTPA, and Feridex.

inside the core since it can produce a long-range magnetic field to promote the spin−spin relaxation process of surrounding water molecules.[8] In this system, 15 nm diameter $MnFe_2O_4$ was used as the core T2 contrast material.[4b] T1 and T2 contrast materials were separated by a layer of SiO_2 with thicknesses of 4, 8, 12, 16, and 20 nm, formed by using a sol−gel reaction (Figure S1).[9] Finally, the T1 contrast material, $Gd_2O(CO_3)_2$ with a thickness of *ca.* 1.5 nm, was deposited on top of the SiO_2 layer by using $Gd(NO_3)_3$ as a precursor (Figures 2a, S2, and S3).[10] Figures 2a and 2b show TEM images of the synthesized DMCA of $MnFe_2O_4$@SiO_2@$Gd_2O(CO_3)_2$. The contrast effects of T1 weighted MR images of the DMCA show significant changes, which are dependent on the thickness of the separating SiO_2 layer. When the thickness of this layer is small and, as a result, the T1 and T2 contrast materials are closely located (e.g., 4 nm), almost no T1 contrast effect is observed (Figure 2c, top). However, as the thickness of the separating layer increases, the T1 contrast dramatically changes from dark gray to bright. Such change is clearly observed in the color coded MR image (Figure 2c, bottom). The relaxivity coefficient, *r1*, which is the value of MR contrast effects, changes in the order 2.0, 4.0, 25.1, 33.1, and 32.5 mM^{-1} s^{-1} as the thickness of the separating layer increases in the respective order 4, 8, 12, 16, and 20 nm (Figure 2e and h). The largest change corresponds to a 16 time increase of the T1 effect. When the thickness of the separating layer exceeds 12 nm, the DMCA shows a strong T1 signal, which is roughly 3 times larger than that of the conventional contrast agent, Gd-DTPA (Gadolinium-diethylenetriaminepentaacetate, Magnevist, *r1* = 9.6 mM^{-1} s^{-1}). Higher *r1* effect of DMCA is possibly caused by its slower tumbling rate compared to the molecular contrast agent.[11] The T1 signal is high when paramagnetic electron spins of the T1 contrast agent are directly in contact with water molecules *via* dipolar interactions between electron spins of the contrast agent and nuclear spins of water.[12] By introducing the T2 nanoparticle contrast agent, however, such coupling processes are perturbed by the additional magnetic field generated. As seen in this case, such effects are tunable by using separating layer between T1 and T2 materials. By controlling the thickness of the separating layer, quenching of the T1 signal by the T2 superparamagnetic core dramatically decreases from 94% to 0% (Figure 2f and Table S1). The T2 contrast gradually changes from black to dark gray as the thickness of SiO_2 increases (Figure 2d). The T2 relaxivity coefficient (*r2*) of the DMCA changes in the order 332, 318, 305, 274, and 213 mM^{-1} s^{-1} as the SiO_2 thickness increases in the respective order 4, 8, 12, 16, and 20 nm (Figure 2g and h and Table S2). In our DMCA model, T2 nanoparticle contrast agent in the core is a magnet which generates a new local magnetic field which is known to be distance-dependent with $1/d^3$ (d = distance from the T2 agent).[13] This magnetic field prompts the transverse T2 relaxation rate of water nuclear spins in the vicinity.[12,14] However, the presence of the SiO_2 layer reduces the magnetic field to the surrounding water molecules, which results in reduced T2 contrast effects with roughly a one third loss of the T2 contrast effect in the case of the 20 nm SiO_2 layer. Even so, all of the DMCAs still have at least two times higher *r2* values compared to the conventional T2 agent, Feridex (iron oxide, *r2* = 108 mM^{-1} s^{-1}). The field dependent dipolar couplings are critical in T1 and T2 signals, and it is observed that electron spin relaxation processes of T1 agents are more susceptible to the attenuation of the local magnetic field.

The DMCA developed in this effort displays dual mode contrast effects, and therefore, it can be used to perform AND logic in MR imaging. In the positive T1 mode, both the DMCA and Gd-DTPA display bright MR signals with "ON" responses while water and Feridex have dark T1 signals with "OFF" responses (Figure 3a). In the negative T2 mode, the DMCA and Feridex display dark signals, which correspond to "ON" states while water and Gd-DTPA show bright T2 signals, which are "OFF" states. Importantly, only the DMCA possesses "ON" states in both imaging modes. Therefore, unlike conventional contrast agents, the DMCA has AND logic, which gives the MR imaging a self-confirmation capability. This feature was demonstrated by performing MR imaging with three separate 1 mm diameter tubings, each containing DMCA, Feridex, and Gd-DTPA, which were implanted in a mouse (Figure 3b). Specifically, the relaxivity change of each imaging mode ($\Delta Ri/Ri_{precontrast}$, $Ri = 1/Ti$; $i = 1, 2$) was measured. Higher Ri indicates

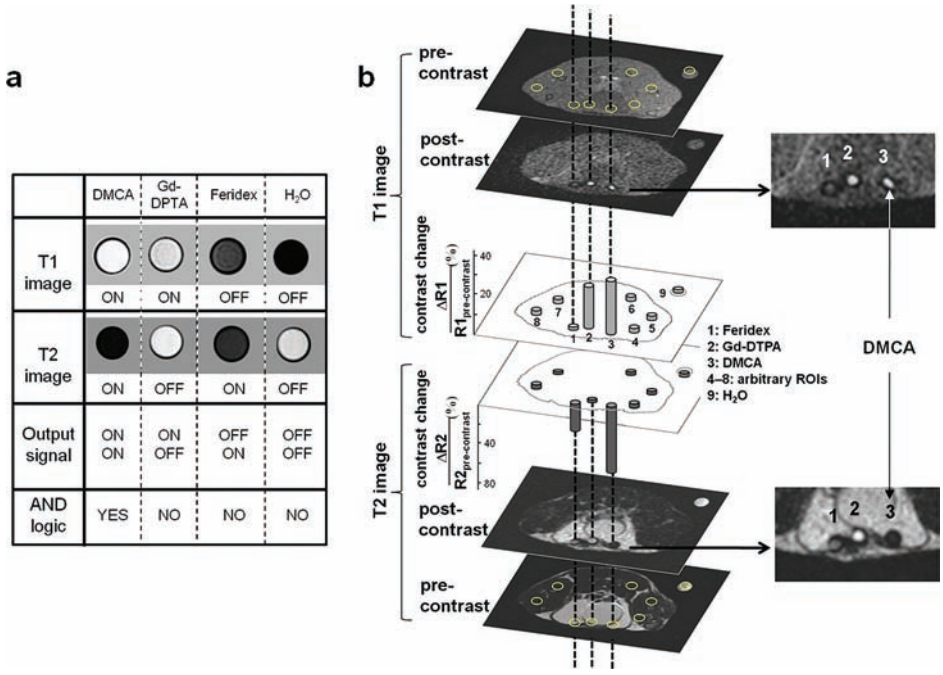

Figure 3. DMCA as an AND logic contrast agent. (a) T1- and T2-weighted MR images of DMCA [$MnFe_2O_4$@SiO_2@$Gd_2O(CO_3)_2$, SiO_2 = 16 nm], Feridex, Gd-DTPA, and water. In T1 mode, the positive (or bright) MR image was the "ON" state, while the negative (or dark) image was the "OFF" state. In T2 mode, the dark image was the "ON" state, while the bright image was the "OFF" state. Only DMCA exhibited the "ON" state in both T1- and T2-weighted images to give its AND logic. (b) T1-and T2-weighted transverse MR images of a mouse where 1 mm diameter tubings containing DMCA, Feridex, and Gd-DTPA were implanted near abdomen. Changes of relaxivity R1 and R2 ($\Delta Ri/Ri_{precontrast}$ (%) = ($Ri - Ri_{precontrast}$)/ $Ri_{precontrast}$; i = 1, 2) were measured for eight different regions of interest (ROI) by comparing pre- and postcontrast images. Higher Ri indicates enhanced contrast effects. In the T1 image, ROI #2 (Gd-DTPA) and ROI #3 (DMCA) exhibited relaxivity change of 30% and 35%. In T2 image, ROI #1 (Feridex) and ROI #3 (DMCA) exhibited a relaxivity change of 35% and 72%. All the other ROIs exhibited minimal signals (~5%) in both T1 and T2 images. Only DMCA exhibited simultaneously high signal in both T1 and T2 to satisfy the "ON" output for AND logic. T1 images were obtained by using a fat suppression sequence, and all images were taken by using 3 T MRI. Contrast agents: 200 μM (Gd) for T1 image, 100 μM (Mn+Fe) for T2 image.

better contrast effects. In the T1 image, region of interest (ROI) #2 (Gd-DTPA) and ROI #3 (DMCA) exhibit a large relaxivity change of 30% and 35%, respectively. In the T2 image, ROI #1 (Feridex) and ROI #3 (DMCA) exhibit a high relaxivity change of 35% and 72%, respectively. All the other ROIs give minimal signal changes in both T1 and T2 images. Among all the ROIs examined, only DMCA shows simultaneously high MR signals in both T1 and T2 modes. As a consequence of the ability to change from bright to dark reversibly leading to "ON" state responses for AND logic, the DMCA can be used to provide self-confirmed imaging. Any faulty "AND" logic can be eliminated by comparing changes between precontrast and postcontrast MR images which will render fault-free MRI capability.

Here, we have a demonstrated core−shell design approach where the degree of T1 and T2 couplings can be modulated by using a separating layer, which makes it possible to create new contrast agents with tunable and maximized T1 and T2 signals. Our DMCA not only has a universal design concept for any T1/T2 combinations but also adopts a synthetic method which is simple and reproducible. The finding suggests that DMCA can be potentially applied to the imaging of a wide range of biological targets with enhanced diagnostic accuracy.

Acknowledgment. We thank Dr. H. S. Kwon and J. K. Kim (KBSI) for TEM analysis, Dr. C. H. Lee (KBSI-Ochang) for MR measurements (4.7 T MRI) and S.-H. Moon (Yonsei Univ.) for providing $MnFe_2O_4$ nanoparticles. This work was supported in part by the CRI (2010-0018286), WCU (2008-9-1955), NCI Center for Cancer Nanotechnology Excellence, LG Yonam Foundation in the program 2008, and 2nd stage BK21 projects for chemistry and medical science.

Supporting Information Available: Detailed information of nanoparticle synthesis and MRI sequences for relaxivity coefficient measurement. This material is available free of charge via the Internet at http://pubs.acs.org.

References

(1) (a) Massoud, T. F.; Gambhir, S. S. *Gene. Dev.* **2003**, *17*, 545–580. (b) Nahrendorf, M.; Zhang, H.; Hembrador, S.; Panizzi, P.; Sosnovik, D. E.; Aikawa, E.; Libby, P.; Swirski, F. K.; Weissleder, R. *Circulation* **2008**, *117*, 379–387. (c) Cheon, J.; Lee, J.-H. *Acc. Chem. Res.* **2008**, *41*, 1630–1640. (d) Gao, J. H.; Gu, H. W.; Xu, B. *Acc. Chem. Res.* **2009**, *42*, 1097–1107.
(2) Lauffer, R. E. *Chem. Rev.* **1987**, *87*, 901–927.
(3) Na, H. B.; Song, I. C.; Hyeon, T. *Adv. Mater.* **2009**, *21*, 2133–2148.
(4) (a) Arbab, A. S.; Liu, W.; Frank, J. A. *Expert Rev. Med. Devices* **2006**, *3*, 427–439. (b) Jun, Y.-w.; Lee, J.-H.; Cheon, J. *Angew. Chem., Int. Ed.* **2008**, *47*, 5122–5135.
(5) (a) Caravan, P. *Chem. Soc. Rev.* **2006**, *35*, 512–523. (b) Bulte, D. L.; Kraitchman, W. M. *NMR Biomed.* **2004**, *17*, 484–499.
(6) Corot, C.; Robert, P.; Idèe, J.-M.; Port, M. *Adv. Drug Delivery Rev.* **2006**, *58*, 1471–1504.
(7) Seo, W. S.; Lee, J. H.; Sun, X.; Suzuki, Y.; Mann, D.; Liu, Z.; Terashima, M.; Yang, P. C.; McConnell, M. V.; Nishimura, D. G.; Dai, H. *Nat. Mater.* **2006**, *5*, 971–976.
(8) McRobbie, D. W.; Moore, E. A.; Graves, M. J.; Prince, M. R. *MRI from picture to proton*; Cambridge University Press: Cambridge, 2003.
(9) Yi, D. K.; Lee, S. S.; Papaefthymiou, G. C.; Ying, J. Y. *Chem. Mater.* **2006**, *18*, 614–619.
(10) Liu, G.; Hong, G.; Sun, D. *J. Colloid Interface Sci.* **2009**, *278*, 133–138.
(11) Caravan, P. *Acc. Chem. Res.* **2009**, *42*, 851–862.
(12) (a) Mitchelle, D. G. *MRI Principles*; Saunders Publishing: 1999. (b) Hashemi, R. H.; Bradley, W. G.; Lisanti, C. J. *MRI: the Basics*; Lippincott Williams & Wilkins: 2004.
(13) Rife, J. C.; Miller, M. M.; Sheehan, P. E.; Tamanaha, C. R.; Tondra, M.; Whitman, L. J. *Sens. Actuators, A* **2003**, *107*, 209–218.
(14) Koenig, S. H.; Kellar, K. E. *Magn. Reson. Med.* **1995**, *34*, 227–233.

JA104503G